NTNU

Norwegian University of
Science and Technology

Alkali - Silica Reactions in Concrete Dams

Alkali Leaching in the Votna Dam

Havvagul Vurucu

Master of Science in Civil and Environmental Engineering
Submission date: June 2016
Supervisor: Klaartje De Weerdt, KT
Co-supervisor: Gilles Plusquellec, KT

Norwegian University of Science and Technology
Department of Structural Engineering

Department of Structural Engineering
Faculty of Engineering Science and Technology
NTNU- Norwegian University of Science and Technology

ACCESSIBILITY

OPEN

MASTER THESIS 2016

SUBJECT AREA: Concrete	DATE: June 10, 2016	NO. OF PAGES: 58

TITLE:

Alkali – Silica Reactions in Concrete Dams: Alkali Leaching in the Votna Dam

Alkalireaksjoner i betongdammer: Utvasking av alkalier i Votna dammen

BY:

Havvagul Vurucu

SUMMARY:
This study focuses on Votna 1 dam, constructed in 1966 – 1968. The dam is a double curved arch dam connected to a slab dam, which is situated in the south – western part of Norway 950 m above sea level. The structure was diagnosed with ASR in 1987 – 1988.

The research question addressed in this thesis is how deep leaching affects the alkali content in in-situ concrete. To the authors knowledge there is currently no data available on this.

The extent of leaching is investigated by measuring the alkali metal profiles in concrete cores using the cold water extraction – method. Concrete cores were retrieved from a selection of locations with different exposure conditions at the slab dam. The extraction method allowed measuring alkali metal leaching in the cores taken from the dam. For submerged and partially submerged exposure, leaching appeared to reduce the alkali content in outer 10 cm of dam. The concrete exposed to rain and the concrete sheltered inside the dam exhibited no clear leaching profiles, but variations in the alkali content starting from 5 cm and going towards the surface were observed. The reason for these variations is still unknown.

RESPONSIBLE TEACHER: Klaartje De Weerdt, NTNU

SUPERVISOR(S): Klaartje De Weerdt, NTNU and Gilles Plusquellec, NTNU

CARRIED OUT AT: Department of structural engineering

Acknowledgements

I would firstly like to thank the post doc and my supervisor Dr. Gilles Plusquellec for all his efforts with my thesis. Besides being a supervisor, he was also a great collaborator. I do not think I would be able to finish the hard "arm-killing" laboratory work and write this thesis without his help and guidance. Thank you for your patience and for always having time to answer my questions. I will also thank my supervisor Associate Prof. Dr. Klaartje De Weerdt for superior guidance and for giving me such motivation and inspiration when working with this thesis. It really means a lot to me, thank you!

A huge thank to Tone Anita Østnor from Sintef for assistance with the process with liquid nitrogen, and to Roger Leistad from Sintef for the help with sawing and crushing of the test materials. I will also thank Jan Lindgård and Hans Stemland from Sintef for taking time to have a meeting with me and talk about ASR. Also a huge thank to the manager of the material laboratory at NTNU, Steinar Seehuus, for showing me how to use the vibratory disc mill and for ordering the liquid nitrogen, and to Syverin Lierhagen for doing the ICP test.

I would also like to thank Prof. Dr. Mette R. Geiker for professional guidance, and Prof. Dr. Terje Kanstad for making it possible for me to write this thesis.

Last but not least, a huge thank to my family and friends for their support and motivation.

Trondheim, June 10, 2016

Havvagul Vurucu

Preface

This master thesis was prepared during spring 2016 at Norwegian University of Technology and Science. The thesis consists of a brief literature study, experimental work and writing of the thesis. All work has been performed during a total of 20 weeks: 5 weeks of literature study, 9 weeks of experimental work in the laboratory and 6 weeks of interpreting results and writing.

During the thesis, I worked in close collaboration with Post Doc Gilles Plusquellec. Gilles' post doc project (2015 – 2017) is about the alkali distribution in ASR affected concrete. This project is on its turn part of a larger project "ASR KPN" (2014 – 2018) partially funded by the Research Council of Norway (RCN project 23661) and managed by Jan Lindgård at SINTEF Building and Infrastructure.

Prior to the master thesis, I have had one lecture briefly on ASR within the course LO264B Building Materials when taking my bachelor degree at Oslo and Akershus University College of Applied Sciences. Except from that, I had never worked with ASR and did not know what leaching of alkalis was. Hence, this master thesis has given me the opportunity to be introduced to a new topic. As my studies up to now mainly have focused on structural design, I have been able to broaden my view and perform research within the field of material science.

In addition, I presented the main findings of my master thesis at "2nd Nordic mini-seminar on Residual service life & capacity of deteriorated concrete structures" 1st and 2nd of June 2016 in Oslo. The extended abstract prepared for this workshop can be found in the appendix.

Abstract

Alkali – silica reaction (ASR) is a common durability problem for concrete. There are three conditions that need to be fulfilled for the reaction to occur: sufficient moisture, alkali reactive aggregates and high alkali content in the concrete. The reaction can lead to alkali-silica gel formation, which can expand when absorbing water. This expansion can lead to a volume increase of the concrete. Consequently the concrete may crack and forces due to constrained expansion may develop.

This study focuses on Votna 1 dam, constructed in 1966 – 1968. The dam is a double curved arch dam connected to a slab dam, which is situated in the south – western part of Norway 950 m above sea level. The structure was diagnosed with ASR in 1987 – 1988.

The research question addressed in this thesis is how deep leaching affects the alkali content in in-situ concrete. To the authors knowledge there is currently no data available on this.

The extent of leaching is investigated by measuring the alkali metal profiles in concrete cores using the cold water extraction – method. Concrete cores were retrieved from a selection of locations with different exposure conditions at the slab dam.

The extraction method allowed measuring alkali metal leaching in the cores taken from the dam. For submerged and partially submerged exposure, leaching appeared to reduce the alkali content in outer 10 cm of dam. The concrete exposed to rain and the concrete sheltered inside the dam exhibited no clear leaching profiles, but variations in the alkali content starting from 5 cm and going towards the surface were observed. The reason for these variations is still unknown.

Sammendrag

Alkali – silika reaksjoner (ASR), som også kalles for alkalireaksjoner (AR) i Norge, er et vanlig problem for betongens holdbarhet. Det er tre betingelser som må være oppfylt for at reaksjonen kan oppstå: tilstrekkelig fuktighet, alkali- reaktive tilslag og høyt alkali-innhold i betongen. Dersom reaksjonen oppstår kan den føre til dannelse av alkali – silika – gel, noe som kan ekspandere ved absorbering av vann. Denne utvidelsen kan føre til en volumøkning av betongen. Følgelig kan betongen risse opp og tvangskrefter som prøver å holde igjen for utvidelsen kan oppstå.

Denne oppgaven fokuserer på Votna 1 dammen, bygget i årene 1966 – 1968. Dammen består av en buedam koblet til en platedam, og ligger i den sørvestlige delen av Norge 950 moh. Konstruksjonen ble diagnostisert med ASR i årene 1987 – 1988.

Problemstillingen for denne oppgaven går ut på hvor dypt utvasking av alkalimetaller påvirker alkaliinnhold i plasstøpt betong. Til forfatterens kunnskap er det per dags dato ingen tilgjengelig data på akkurat dette.

Det har blitt boret ut betongkjerner fra et utvalg av steder på platedammen med ulike eksponeringsforhold. Omfanget av utvaskingen har blitt undersøkt ved å måle alkalimetall – profiler i de utborede betongkjernene ved hjelp av en ekstraksjonsmetode.

Ekstraksjonsmetoden ser ut til å egne seg til å måle utvasking av alkalimetaller i betongkonstruksjoner. For eksponering både permanent og delvis under vann ser det ut til at utvaskingen har redusert alkaliinnholdet i ytre 10 cm av dammen. Betongen utsatt for regn og betongen skjermet inne i dammen hadde profiler der ingen tydelig utvasking ble indikert, men det ble observert variasjoner i alkaliinnholdet fra 5 cm dybde og utover mot den eksponerte overflaten. Årsaken til disse variasjonene er fremdeles ukjent.

Table of content

List of figures

List of tables

1. Introduction

Concrete is a composite material made out of cement, aggregates (coarse and fine) and water. Cement is a hydraulic binder, which means that it will give solid reaction products when reacting with water. This reaction is called hydration. The main hydration product, or hydrate, of portland cement is the calcium silicate hydrate, also called the C-S-H (see equations 1 and 2). It gives the concrete its strength, stiffness and durability. Another hydrate is the portlandite, or calcium hydroxide $Ca(OH)_2$. It contributes to give a high pH to the pore solution (Opsahl et al., 2005).

The reaction formula for hydration of tricalciumsilicate (Johansen, 2009):

$$2(3CaO{\cdot}SiO_2) + 6H_2O \rightarrow 3CaO{\cdot}2SiO_2{\cdot}3H_2O + 3Ca(OH)_2 \quad (1)$$

The reaction formula for hydration of dicalciumsilicate (Johansen, 2009):

$$2(2CaO{\cdot}SiO_2) + 4H_2O \rightarrow 3CaO{\cdot}2SiO_2{\cdot}3H_2O + Ca(OH)_2 \quad (2)$$

The pore solution is contained in the pores of the hardened concrete, mortar or paste. There are a lot of pores. Some of these are empty, while others are completely or partially filled. The solution in the pores (i.e. pore solution) is highly basic: pH > 12.5 for a hydrated portland cement. It is essentially composed of dissolved alkali metals and hydroxides (K^+, Na^+ — OH^-) (Diamond, 1989), but also of other elements (e.g. Ca, Mg, Si, Al, Fe and S) (Andersson et al., 1989) in smaller concentrations. The high alkali metals concentration contributes to the high pH of the pore solution (pH higher than 12.5).

The pH of the pore solution is also affected by external factors. For example, ions may leak if the hardened material is in contact with an external source of water (e.g. rain). The process is called leaching and is a diffusion – reaction phenomenon (Rozière et al., 2009), and lead to a decrease of the concentration of the alkalis metals ions in the pore solution, which means that the pH will also decrease (Plusquellec et al., 2016).

The environment of high pH advantageously makes the steel reinforcement more resistant against corrosion (Andrade et al., 1995), but it can also make the reactive aggregates dissolve.

The reactions are known as alkali – aggregate reactions (AAR), which can provoke premature distress and reduce the service life of concrete structures. AAR can be divided into two types that are most common: alkali – carbonate reaction (ACR) and alkali – silica reaction (ASR) (Fournier and Bérubé, 2000). This study only involves the latter.

1.1. Alkali – Silica Reaction

In Norway, one of the main deterioration mechanisms in concrete is ASR (Larsen et al.). ASR occurs only if three conditions are fulfilled simultaneously: sufficient moisture content, reactive aggregate and high alkali content of concrete (Figure 1.1). If one of these three conditions is absent, the reaction will not take place (Lingård et al., 2015).

The Norwegian reactive aggregates are generally slowly reactive. The slow rate of the reaction could be due to the cold climate. In this condition, it generally takes at least 10 – 15 years to see visible signs of ASR on concrete structures (Lingård et al., 2015). Other parameters affecting the rate of ASR could be the composition of the aggregates and the cement.

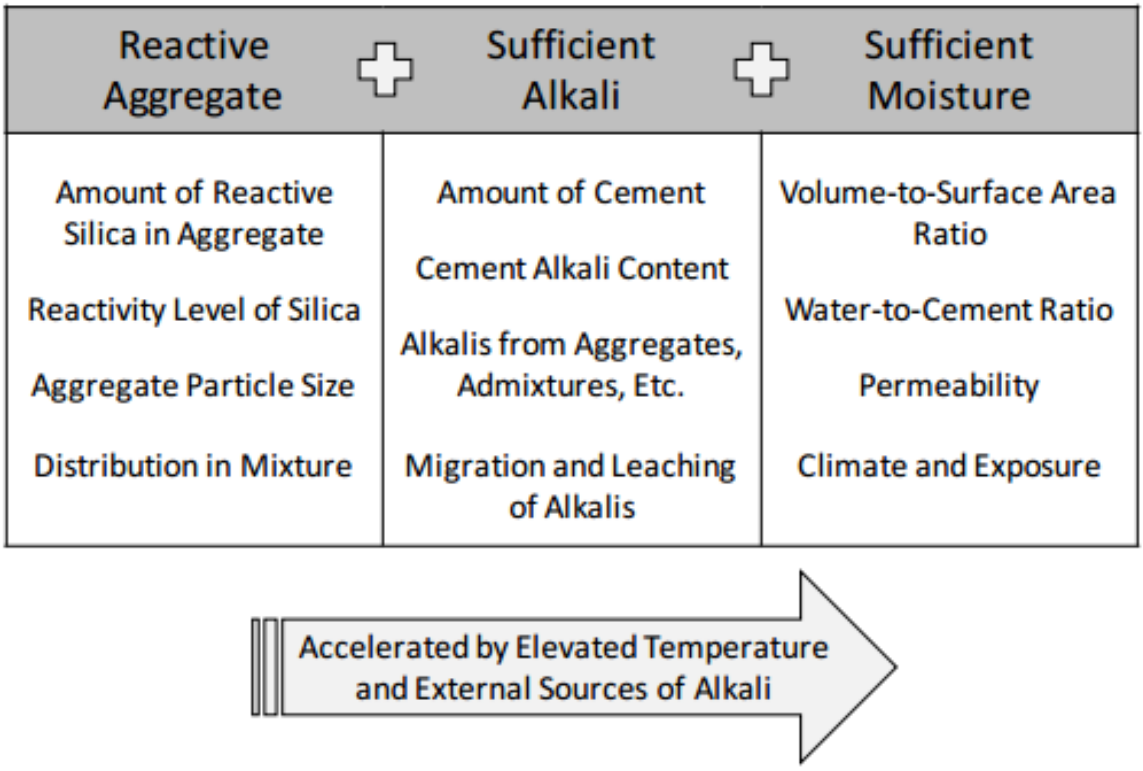

Figure 1.1: Three necessities of ASR (Deschenes et al., 2009)

During ASR, the high alkali content, and consequently the high pH of the pore solution can lead to the dissolution of the siliceous phase of the aggregates, followed by the precipitation of a gel. The process of alkali gel formation can briefly be written as (Pan et al., 2012):

$$\equiv Si - O - Si \equiv + R^+ + OH^- \rightarrow \equiv Si - O - R + H - O - Si \equiv$$

The R^+ is representing an alkali ion (i.e. sodium (Na^+) and potassium (K^+)). The silicic acid that is produced simultaneously with the alkali-silica gel will continue reacting with further hydroxyl ions (Pan et al., 2012):

$$\equiv Si - O - H + R^+ + OH^- \rightarrow \equiv Si - O - R + H_2O$$

After the precipitation, the alkali – silica gel diffuses away from the aggregate into the pores. Then it reacts with calcium ions (Ca^{2+}), and forms an alkali-calcium-silicate hydrate gel (Dron and Brivot, 1992, Dron and Brivot, 1993, Diamond, 2000). The gel may absorb water and swell, leading to an increase of its volume and to expansion of the concrete itself. The reaction of the expansion of the gel is given as (Pan et al., 2012):

$$\equiv Si - O - R + nH_2O \rightarrow \equiv Si - O^- - (H_2O)_n + R^+$$

where *n* is the number of hydration.

The expansion of the concrete will create tensile stresses, and if the stresses exceed the tensile strength of the concrete, the concrete cracks (Figure 1.2). It is assumed that the gel permeates into the cracks (Multon et al., 2009). The crack pattern, called “map cracking” (Hagelia, 2004), is characteristic for ASR (Figure 1.5). It is also possible that the expansion stops quite early before causing any cracks. In this case, it is harder to discover the ASR. The expansion can decrease the durability of the concrete even though the cracks have been avoided. This can be due to forces developed due to restrained expansion.

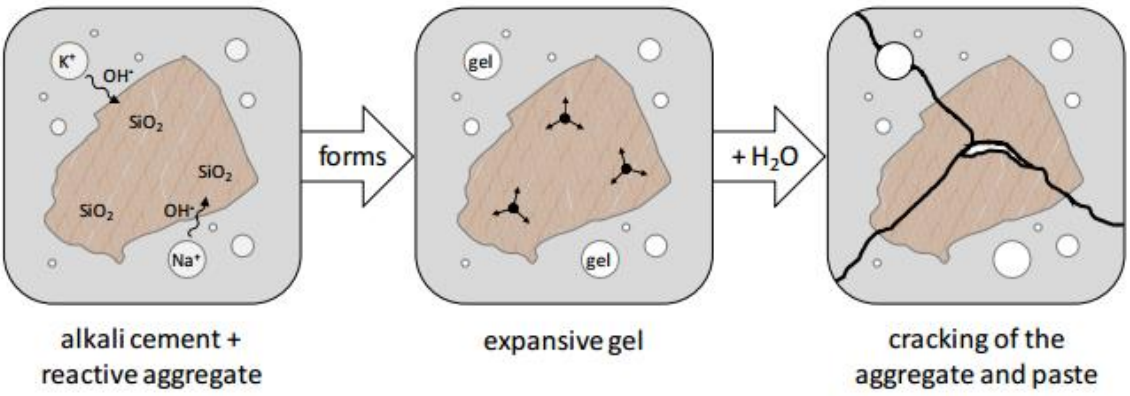

Figure 1.2: Alkali - silica reaction process (Deschenes et al., 2009)

Alkali Silica reaction is a very common durability problem for concrete. Structures in humid climate are the most vulnerable, like dams, bridges and hydraulic structures. Other examples of structures ASR can damage are walls, barriers, pavements and nuclear/power plant structures (Rajabipour et al., 2015).

1.2.Methods to measure the alkali content in concrete

The durability of concrete is mainly governed by the pH of its pore solution. The pH is strongly related to the free alkali content of the concrete. It is thus of first importance to measure this latter, and different methods can be used.

The most common method is the pore water expression (Longuet et al., 1973, Barneyback and Diamond, 1981) and consists of compressing the hardened material (paste, mortar or concrete) with a high pressure equipment. This results in the expression of the pore solution, which can be analyzed. The applicability of the pore water expression is however limited by the potentially low amount of free water available, especially for old samples. For hardened concrete, the high content of coarse aggregates is also challenging. In addition, this method implies to know the amount of free water in the sample in order to determine the free alkali content (Plusquellec et al., 2016). Pore water expression is thus not applicable in this study due to the age of the analyzed concrete.

The in situ leaching is another available method. It consists of drilling small cavities (diameter: 3 to 5 mm; deep: 25 to 35 mm) from the surface of the sample, adding a known

amount of deionized water in the cavities. The solution in the cavities can be analyzed when the equilibrium is reached (approx. 2 weeks) (Sagüés et al., 1997, Li et al., 1999). However, this method needs to be performed on water saturated samples. All saturation methods may lead to a leaching of alkali metals (Bokern, 2008, Lindgård, 2013b), which will invalidate the results. In situ leaching is also a time consuming method. As a result, this method is also not suitable here.

Finally, ex situ leaching methods can also be used to determine the free alkali content. 3 variations can be found in the literature: "cold water extraction" (Alonso et al., 2012, Castellote et al., 2001, Li et al., 2005, Pavlik, 2000), "hot water extraction" (Bérubé et al., 2002b, Bérubé et al., 2002a) and "espresso" (Fournier et al., 2016). They all rely on the same principle: the hardened material is ground to powder, and then introduced to a known amount of deionized water (at room temperature or boiling) for a certain amount of time. The obtained suspension is filtrated and the solution can then be analyzed for alkali metals. These methods can be used on relatively dry samples, no water saturation is required and the knowledge of the free water content is not required for a proper estimation of the free alkali content. Among those 3 methods, cold water extraction is the simplest and fastest one (Plusquellec et al., 2016), and is thus used in this study. A detailed description is provided in the section 0 of the present document.

1.3. Votna Dam

The Votna dams are situated in the south – western part of Norway 950 m above sea level. There are four dams owned by Hydro Energy Production AS. They were constructed in the years 1964 – 1966, and form the intake reservoir for the Novle Power Plant. This study focuses on the main dam, Votna 1, which is a double curved arch dam connected to a slab dam (Figure 1.3 and Figure 1.4), with a total length of 185 m and maximum height at 55 m. The thickness decreases from 4 m at the bottom to 0,95 m at the top for the arch, while the slab has a thickness that decreases from 70 – 80 cm at the bottom to 30 cm at the top (Lindgård et al., 2015). The second dam, Votna 2, is a concrete slab dam while the two other dams at Votna are just gravity dams creating the spillway sections. The water level at the reservoir is regulated each year for about 20 m, where it is high during summer/autumn and low during the winter (Larsen et al.).

Figure 1.3: Sideview of Votna 1 – May 2015 (Photo: G. Plusquellec)

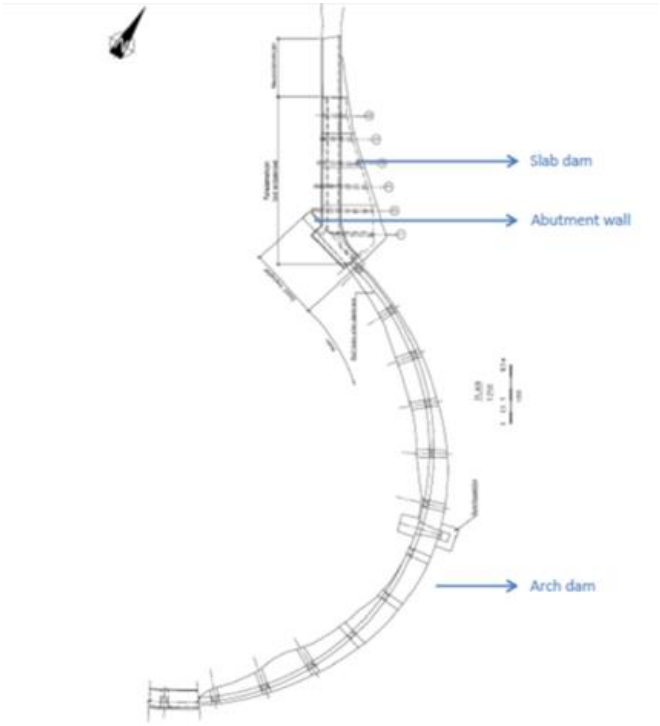

Figure 1.4: Sketch from the top view of Votna 1 (Lindgård et al., 2015)

1.3.1. Background

It was in the years between 1987 and 1988 that Votna 1 was diagnosed with ASR. The typical map cracking pattern was observed (Figure 1.5), and after investigation of the concrete one could confirm that ASR had started. The results from regularly deformation measurements made once a year from 1990 to 2003 at the top of the arch dam showed that an expansion of the concrete was increasing linearly with time (Larsen et al.). High tension occurred in the concrete due to the deformation at the connection point between the arch dam, the abutment wall and the slab dam (Figure 1.4) (Lindgård et al., 2015). Recent inspection in May 2015 also revealed the presence of the alkali silica gel (Figure 1.6).

Figure 1.5: The typical map cracking pattern at Votna 1 - May 2015 (Photo: G. Plusquellec)

Figure 1.6: Presence of alkali silica gel at Votna 1 - May 2015 (Photo: G. Plusquellec)

1.4. Objective and hypothesis

The primary objective of this study is to check the applicability of the selected method to measure the free alkali content. The secondary objective is to understand the possible influence of the different exposure conditions on the free alkali metals content in the concrete. Samples were taken from the Votna 1 slab dam at various locations. Depending on the location, it is expected to observe different evolutions of the leaching (Figure 1.7). Core I and III were only exposed to water, while II was exposed to both water and air due to the different water levels during a year. Core VI was only affected by rain exposure, while core VII was sheltered inside the dam.

The hypothesis is that leaching of alkalis will reduce the alkali content of the pore solution (Figure 1.7). Core I and III are assumed to present the most intensive leaching, since they are permanently submerged. The most intensive leaching is expected to have a leaching depth around 5 cm from the exposed surface. It is assumed that core II have less leaching, which indicates a smaller leaching depth, than the submerged cores I and III. Core VI is expected to suffer the least from leaching, while core VII should not present any leaching as this core has no exposure to water.

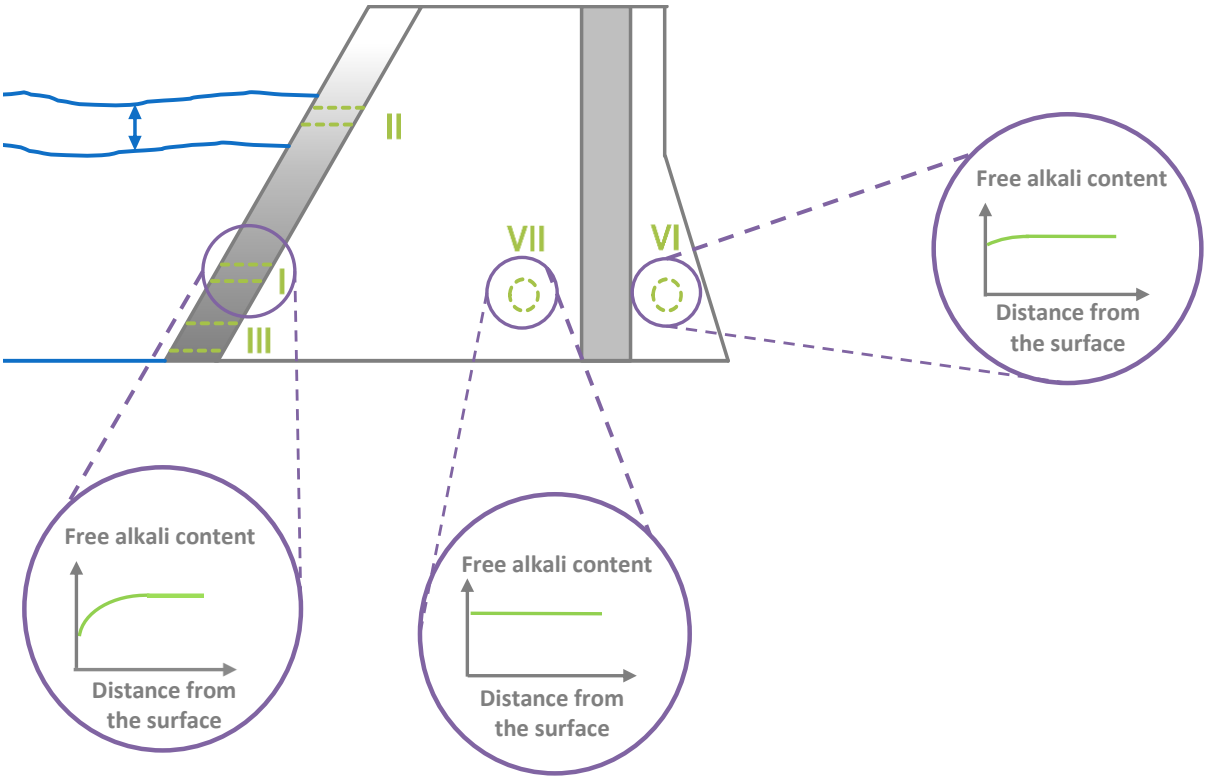

Figure 1.7: Side view of the slab dam with the expected alkali distribution from the different exposure conditions (Source: G. Plusquellec).

To the author's knowledge, the extent of leaching in a dam has not been investigated before. This is due to the difficulties with emptying a dam, also considering that there were no any good methods to measure the free alkali content in in – situ concrete.

2. Experimental

2.1. Materials

Jan Lindgård (KPN project leader, SINTEF), Gilles Plusquellec (Post Doc NTNU), and Klaartje De Weerdt (supervisor NTNU) visited together with Sjur Åge Ekkje (Hydro Energy) the Votna 1 dam on Wednesday the 5th of May 2015, in order to decide where the samples should be taken. As the dam was rehabilitated during summer 2015, the water reservoir was empty for allowing the repair work. The positions of the samples are indicated on Figure 2.1 and Figure 2.2. Each location is given a "position number" (from I to VIII). The cores taken from the slab dam (positions I, II and III) and the pillar (positions VI and VII) were allocated to this study. The cores were drilled during June 2015 (Figure 2.3). Immediately after drilling, they were labeled with the position and sample number, and wrapped with plastic. Upon receiving, all the cores were stored wrapped at 5°C until analysis. The name, position, diameter and length on each core studied here are provided in Table 2.1. It has to be noticed that the cement used for the slab and the pillar may be different.

Table 2.1: Description of the studied cores.

Name	Position	Diameter (mm)	Length (mm)	Observation
I-14	Slab dam - bottom	150	705	ASR gel
II-13	Slab dam - up	150	630	ASR gel
III-7	Slab dam - bottom	150	200	ASR gel
VI-2	Pillar - outside	95	480	Going through the pillar
VII-5	Pillar - inside	95	480	Going through the pillar

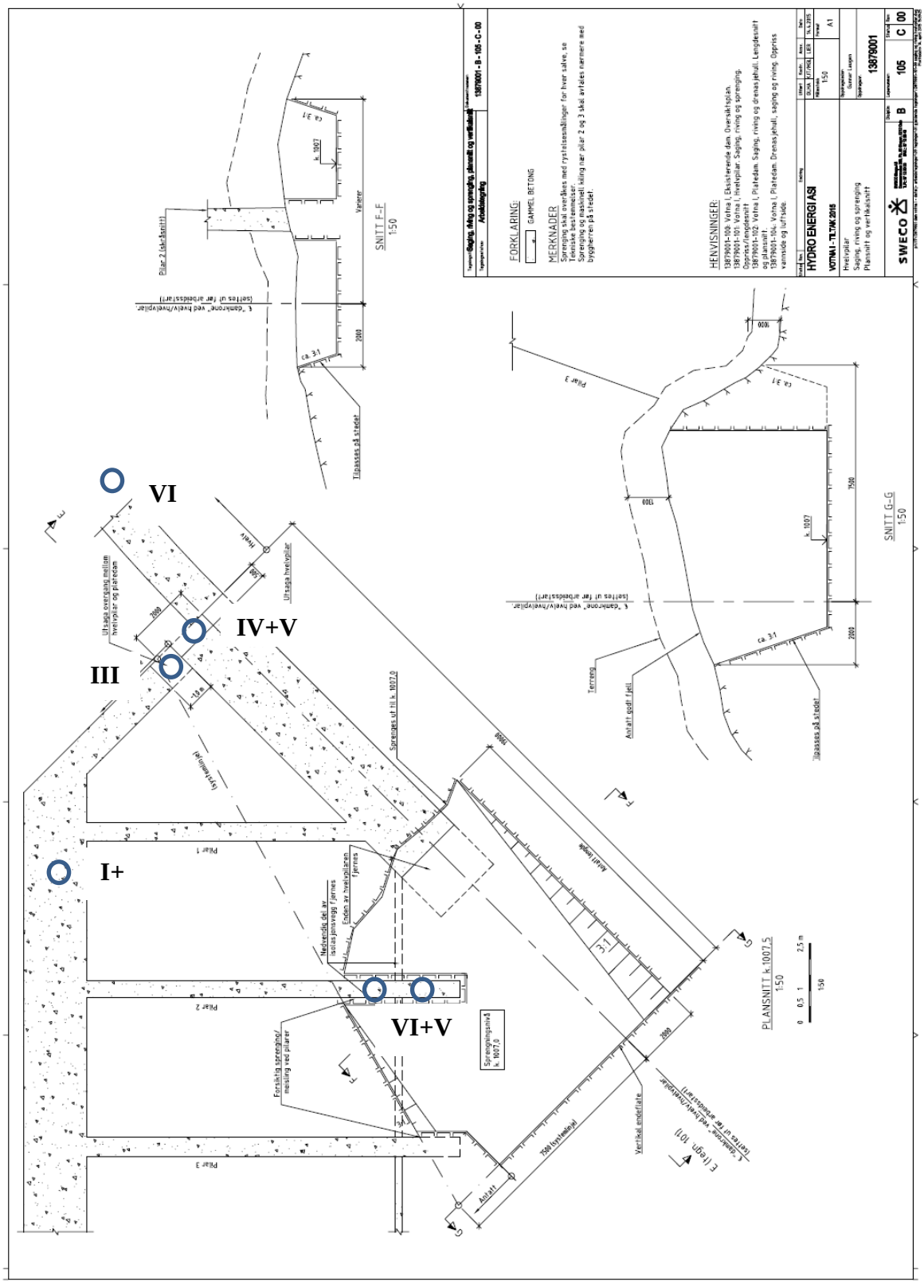

Figure 2.1: Sketch of the slam dam and the abutment wall. The blue circles represent the localization of the samples (Lindgård et al., 2015).

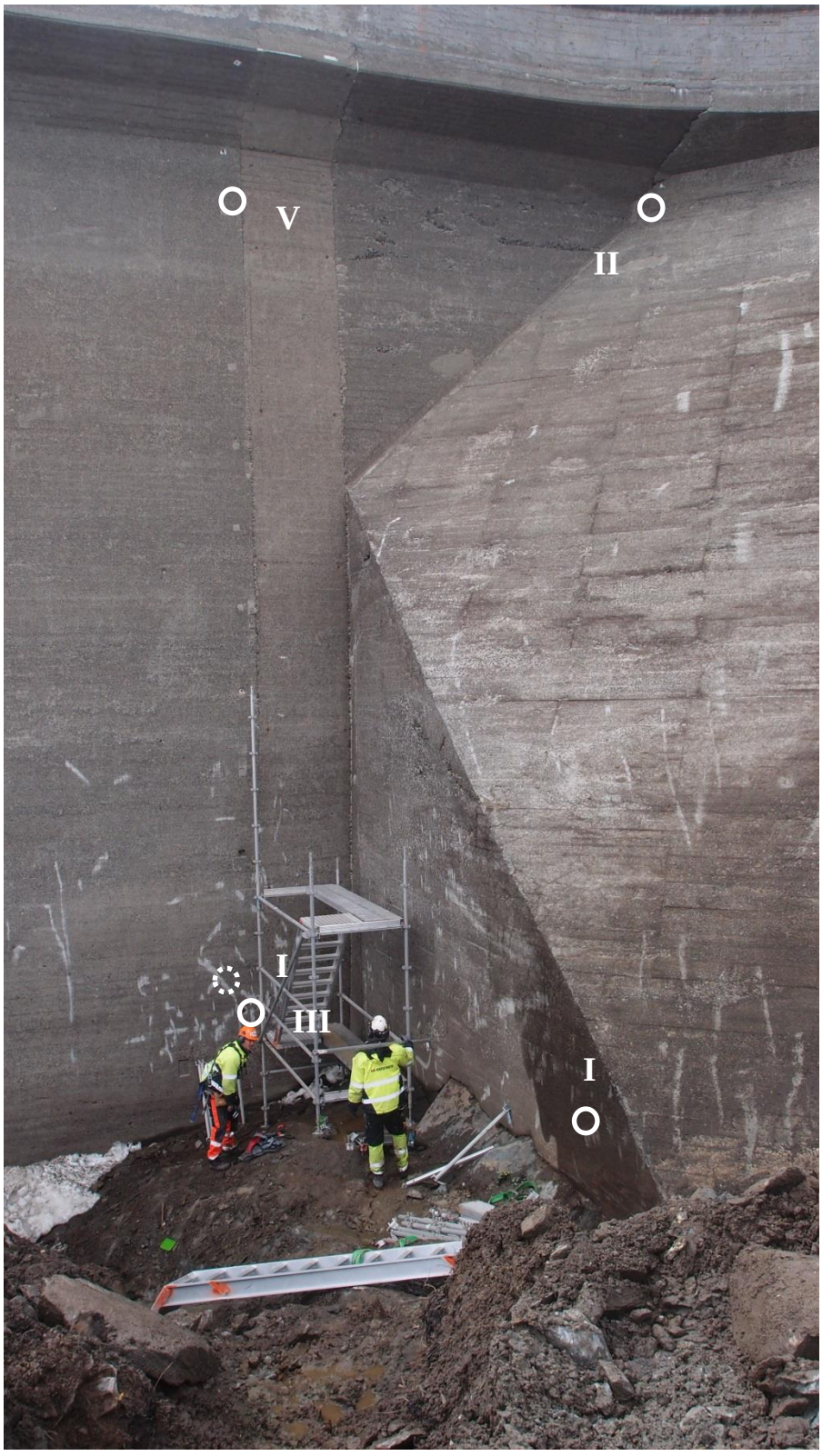

Figure 2.2: Upstream face of the connection point between the arch dam, the slam dam and the abutment wall (Lindgård et al., 2015).

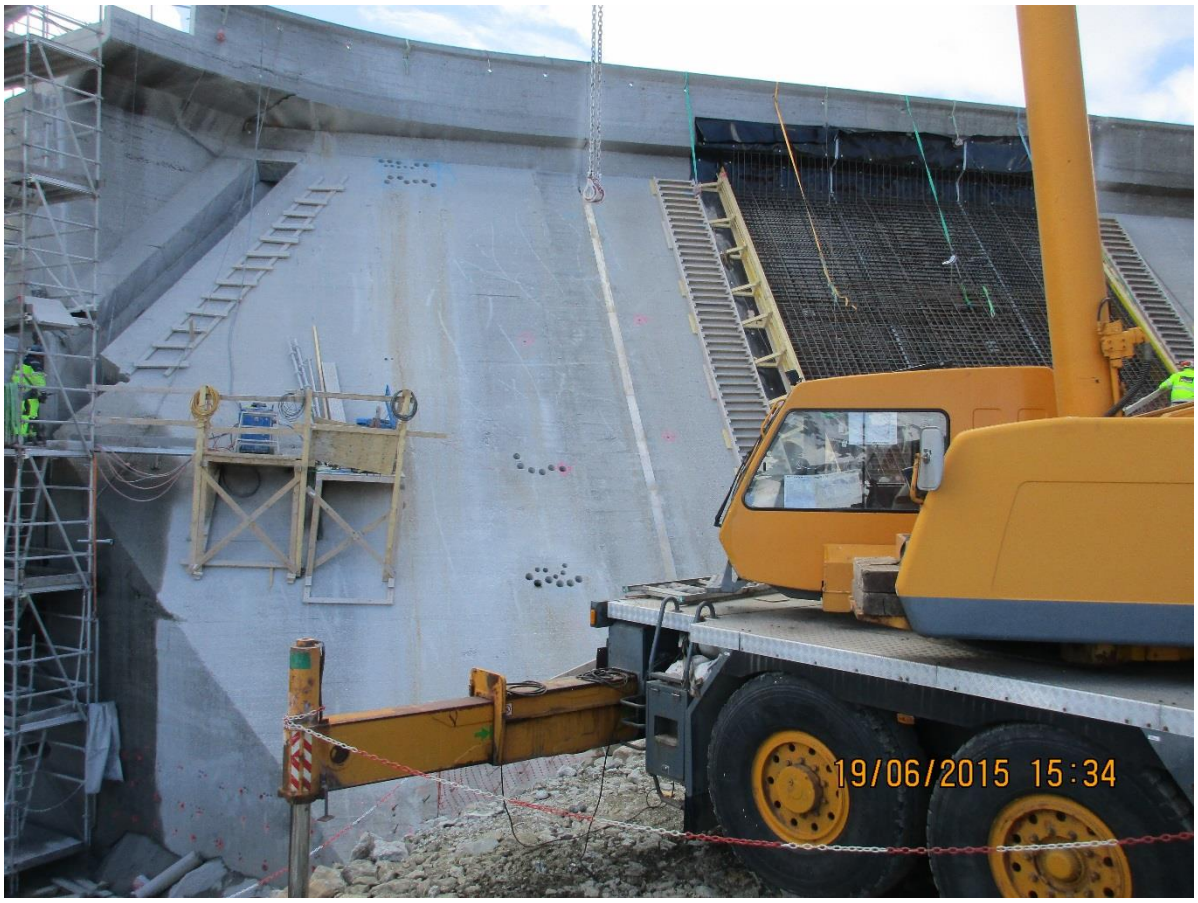

Figure 2.3: Slab dam after drilling (Provided by J. Lindgård).

The samples used for the separation of aggregates (see 2.4 The aggregate separation) was taken from large blocks cut from the slab (Figure 2.3). The coarse aggregate is originally from a local reactive rock, while the origin of the sand is different (Lindgård et al., 2015).

2.2.Sawing and grinding

The cores taken from different locations of the dam were prepared firstly by marking the slices which were going to be analyzed (Figure 2.4). Figure 2.5 is showing the principle of slicing, as the slices needed to be taken from different depths of the cores in order to determine at which extend the leaching occurs.

Figure 2.4: After the marking (Photo: G. Plusquellec).

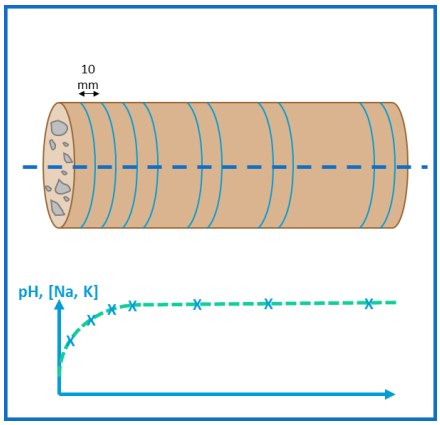

Figure 2.5: The principle of slicing (by G. Pusquellec).

After the marking, the cores were sent to Sintef for sawing and further crushing by a jaw crusher. The sawing was done with a diamond blade, and a minimum amount of cooling water was used during the sawing process, to avoid leaching as much as possible. The discs were crushed with a jaw crusher, and collected in sealed plastic bags, and numbered. The bags were then stored in a desiccator with soda lime at the bottom to avoid carbonation. The next step was to finely grind the crushed slices. In this study, the grinding was done with a vibratory disc mill RS200 from Retsch (1500 rpm during 30 seconds). The powder was then collected from the grinding elements, and put in new sealed plastic bags to be stored in a desiccator.

Figure 2.6: The grinding process (Photo: H. Vurucu).

2.3. Cold Water Extraction

The method used in this analysis is cold water extraction (CWE), also called "ex situ leaching" (Plusquellec et al., 2016). The goal of this method is to measure the free alkali content of a cement paste, mortar or concrete. A known amount of the powdered sample (particles size < 80 µm) is mixed with the same weight of deionized water for a certain amount of time to make the extraction. In this study, 20 g of the ground powder was mixed in a 100 ml beaker with 20 g of deionized water (liquid/solid ratio 1.0) using a magnet stirrer for 5 minutes. The next step is to separate the liquid from the solid by filtration and then finally analyze the solution, also called the extracted solution, for Na and K (Plusquellec et al., 2016). The filtration of the suspension was done with 8 µm Whatmann filter paper, grade 40, using a filtration unit (Figure 2.7). For safety reasons the entire procedure was performed in a fume cabinet.

Figure 2.7: The filtration during CWE (Photo: H. Vurucu)

Ca can also be measured by using methanol instead of deionized water during the extraction in order to avoid the dissolution of portlandite (Plusquellec et al., 2016). In this case 10 g of the ground sample was mixed with 10 g of methanol using the same procedure as described above.

All the extracted solutions were diluted with deionized water (1:10 for CWE with deionized water and 1:100 for CWE with methanol) and acidified (0.1 M of HNO_3) to avoid carbonation

before the elemental analysis. The latter were done by Inductively Coupled Plasma Mass Spectrometry (ICP-MS) with Element 2 Thermo Scientific by Syverin Lierhagen (NTNU).

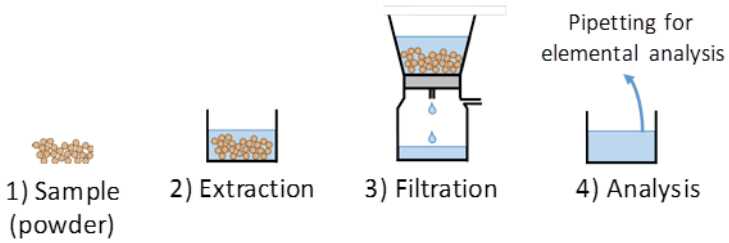

Figure 2.8: Principle of the CWE (by G. Plusquellec)

The free alkali content is determined directly from the results obtained by ICP and is expressed in mmol/mass of sample.

The free water content has been measured by Sintef using the PF method (Sellevold and Farstad, 2005, Plusquellec et al., 2016).

2.4. The aggregate separation

In order to measure the potential release of alkali metals from the aggregates during CWE, the aggregates need to be analyzed separately. If the aggregates release a considerable amount of alkali, it will influence the measurement of the free alkali content in the pore solution.

The first step of this separation method was to cut a concrete block into smaller samples, approx. 10*10*10 cm, and immerse them in water for minimum 3 days to fill the pores with water. After the saturation, the samples were frozen rapidly in order to provide a rapid expansion of the water in the pores. This step was done by putting the samples in liquid nitrogen (temperature -196^{o}C). The samples were then shock heated in the microwave (7 min heating at maximal power). This freeze/thaw process was repeated 3 times for each sample, creating cracks in the concrete (Figure 2.9). Simple hammering was then enough to separate the coarse aggregates from the mortar (Figure 2.10). Finally, the aggregates were washed in a diluted HCl solution. The goal was to completely remove the cement paste from the aggregates (Haugen et al., 2004).

Figure 2.9: The freeze/thaw process using liquid nitrogen and microwave (Photo: H. Vurucu)

Figure 2.10: Hammering to separate the coarse aggregates from the mortar (Photo: G. Plusquellec)

The coarse aggregates were then ground into powder with a vibratory disc mill and the alkali release was checked by CWE, as described earlier.

XRF was performed, using a Bruker S8 Tiger, 4kW x – ray spectrometer, to measure the composition of the aggregates, i.e. the total alkali content.

Another analysis performed was the µXRF to be able to visualize more specifically the alkali in the aggregates. This analysis was done on the water side of the dam for a 28 mm x 19 mm area using Orbis PC µXRF by Edax.

3. Results and discussion

3.1. Alkali release from aggregates

From µXRF analyses one could clearly see the distribution of alkali in the aggregates. While the sodium ions (Na^+) were spread everywhere over the analyzed area, the potassium ions (K^+) were seen more concentrated in the aggregates (Figure 3.1).

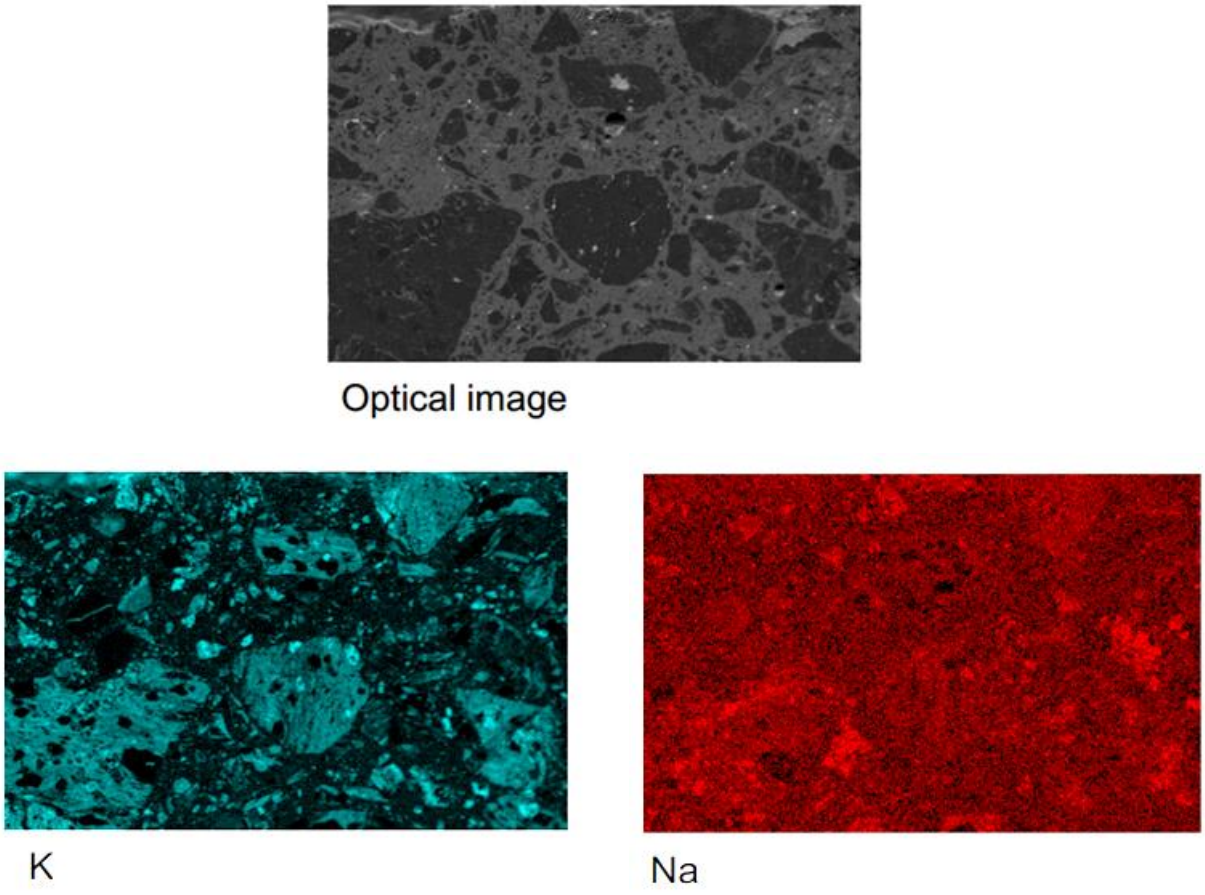

Figure 3.1: The optical image and µXRF analyses of K and Na (Provided by G. Plusquellec).

The aggregates were analyzed separately with XRF, and the total alkali content of the aggregates is shown in Table 3.1. Table 7.1 in the appendix shows the entire composition.

Table 3.1: The total alkali content of the aggregates from XRF-analysis

Constituent	Amount (%)
K_2O	5.00
Na_2O	2.86

By using the molecular mass of sodium, potassium and oxygen (see Table 7.2 in appendix 2), the concentration of sodium and potassium from the XRF – analysis was calculated.

Table 3.2: Composition of the alkali ions in the aggregates from XRF-analysis

The alkali ion	Composition from XRF (mmol/g)
K	1.06
Na	0.92

The results from the calculated release (see appendix 3) from CWE are shown in Table 3.3 below.

Table 3.3: The alkali release from CWE of the aggregates

The alkali ion	Release from CWE (mmol/g)
K	0.005
Na	0.005

The results from Table 3.2 and Table 3.3 are both given in mmol/g. It is possible to see that the release constitutes around 0.5 % of the total content for the both alkali ions.

The total alkali release from CWE is 0,01 mmol/g of aggregate ([Na] + [K]). The concrete from Votna 1 contains ≈ 40 % of coarse aggregates (see appendix 4), thus the calculation for 20 g concrete will give 8 g of coarse aggregate. Mixed with 20 g water as used in these analyses, the result for released alkali will be:

$[Na + K]_{aggregate} = (0.01 \times 8)/0.02 = 4$ mmol/l

In comparison, 20 g of CEM I mortar will give (Plusquellec et al., 2016):

$[Na + K]_{mortar} \approx 50$ mmol/l

This means that the aggregates contribution in the CWE test is at least 10%. This should be kept in mind when analyzing the results.

3.2. Analysis of the cores

In order to measure the alkali content, the idea was to divide the cores lengthwise in two. The aggregates were initially going to be removed from one half to be able to analyze the core both with and without the aggregates included. However, this seemed to be a very challenging task since the aggregates could only be removed by hammering. The separation method using liquid nitrogen (see paragraph 2.4) could not be performed in this case due to the risk of extraction of alkalis from the paste when immersing in water. Hence, when interpreting the results obtained on the concrete cores, one should just keep in mind that part of the alkali can originate from the aggregates.

Figure 3.2, Figure 3.3, Figure 3.4, Figure 3.5 and Figure 3.6 show the ICP results for the different investigated cores. The x-axes represent the depth from the exposed surface into the concrete core. The vertical axes represent the content of Na, K and Ca in mmol/kg concrete.

Figure 3.2 shows the results for the shortest core; core III-7, which was 300 mm and permanently submerged. This core was originally 840 mm, but only the first 300 mm from the exposed surface was received for this study. The slice marked at the deepest point of the core in a distance between 168 mm and 182 mm from the exposed surface was not analyzed (see appendix 5 Figure 7.1), as the originally assumption was that the depth of leaching would not be more than 5 cm from the exposed surface. The analyzed and obtained results for this core are therefore only up to 150 mm. The graph shows that the alkali content is decreasing over the entire analyzed length of the core towards the exposed surface, which indicates leaching. The calcium content is increasing. The results for the analyzed part of core III-7 might go towards a plateau, but this is unclear as the analyzed core is a part of a longer core. Hence, the exact depth of the leaching cannot be measured here.

Figure 3.3 shows the data for the core I-14 which was also permanently submerged, however at a slightly lower depth than core III-7. The total length of core I-14 was 705 mm (see appendix 5 Figure 7.2) and the entire core was analyzed. In the obtained results shown in Figure 3.3, similar trends are observed as for core III-7. However, for core I-14 a plateau of the Na, K and Ca content is observed between 10 and 45 cm depth. Figure 3.3 shows clearly that the alkali content is decreasing towards the exposed surface from a distance around 10 cm. This indicates that leaching affects the alkali concentration up to 10 cm depth from the exposed surface. There is a smooth leaching profile. The results at between 60 and 70 cm

from the exposed surface shows a lower content of Na and K, and higher content of Ca compared to the plateau values. The reason for this is still unclear.

The ICP results of the partially submerged core II-13 (Figure 3.4) also indicate the presence of a plateau as for the previous core I-14 (Figure 3.3), and a similar depth affected by leaching. The plateau is observed between 10 and 40 cm depth. The entire core with a length of 630 mm (see appendix 5 Figure 7.3) was analyzed up to 500 mm. A steep curve showing the decrease of alkalis is observed between 5 cm and 10 cm from the exposed surface (Figure 3.4). The alkali content is also decreasing in a depth from 5 cm towards the exposed surface, but a slight increase is observed at 5 cm depth. The reason for this increase is still unclear. It is assumed that the increase is caused by the different water levels during a year, leading to the concrete being either submerged or exposed to air. The different exposures will cause wetting and drying of the concrete and will lead to movement of ions. The calcium concentration on the other hand is very low at this point around 5 cm from the exposed surface. However, a steep increase in calcium is observed from 5 cm depth towards the exposed surface.

Figure 3.5 shows the ICP results for core VI-2 exposed to rain. The entire length of this core was 480 mm and only up to 43 cm was analyzed (see appendix 5 Figure 7.4). The alkali concentration is decreasing towards the surface, but the concentration up to 5 cm depth from the exposed surface is unclear. There is a remarkable decrease of the alkali content towards the surface between 5 and 10 cm. An indication to the presence of a plateau between 10 cm and 32 cm is observed both for the alkali and the calcium concentration. There is an increase in the calcium concentration starting from 10 cm depth and going towards the exposed surface up to 4 cm depth. The obtained ICP results for this core exposed to rain show lower alkali content in the concrete than the previous analyzed cores from the slab. The reason can be the use of different concrete for this location i.e. supporting pillar, compared to the slab.

The obtained ICP results for core VII-5 which was sheltered inside the dam are shown in Figure 3.6. The core had a total length of 480 mm, and the length up to 43 cm has been analyzed (see appendix 5 Figure 7.5). The hypothesis for this location was a stable alkali content without a decrease towards the exposed surface, indicating no leaching. The results on the other hand show tendency to a decrease of the alkali content towards the exposed surface, but the obtained results from the outermost point at the surface seem to be similar to the concentration of alkalis from the bulk concrete, thereby indicating no leaching. If there was

leaching, the concentration for the outermost point should also be decreasing in accordance with the other points towards the exposed surface. The decrease of alkali content in a depth between 1 and 5 cm from the surface can indicate that there were more aggregates in the concrete composition at this depth which lead to less paste and therefore fewer alkalis. The alkali concentration between 1 and 5 cm seems to be similar to the alkali concentration at the same depth for the rain exposed core VI-2 (Figure 3.5). Figure 3.6 do show a presence of a plateau for core VII-5 between 10 and 43 cm, as the alkali concentration does not have any remarkable decreases. The calcium concentration has a steep increase towards the surface between 2 and 5 cm depth, but the concentration decreases dramatically from 2 cm towards the outermost point of the core.

The cores in Figure 3.3, Figure 3.4 and Figure 3.5 indicate a drop in the other end which is not exposed to water. The reason for the drop can possibly be due to carbonation as the cores are exposed to air on the other end. This is just an assumption, and further investigation on this is needed.

The submerged and partially submerged cores have profiles indicating leaching (Figure 3.2, Figure 3.3 and Figure 3.4). The leaching profiles are dependent on the exposure conditions. Figure 3.3 shows a very smooth leaching profile for the permanently submerged core I-14, and it is possible to see that the other permanently submerged core III-7 (Figure 3.2) also shows a tendency to a smooth leaching profile. The partially submerged core II-13 (Figure 3.4) indicates a clear leaching profile, but there are some variations around 5 cm from the exposed surface. These variations can be caused by the exposure conditions, as this core was exposed to either water or air due to different water levels. Hence, the profile is not as smooth as the permanently submerged core I-14 (Figure 3.3) in comparison. Core VI-2 (Figure 3.5) which was exposed to rain and core VII-5 (Figure 3.6) sheltered inside the dam do not show any leaching profiles. As mentioned, the alkali content is decreasing towards 5 cm from the exposed surface. From 5 cm and towards the outermost points at the surface, some variations are observed. The reason for these variations is still unknown.

Another very interesting observation is that the Ca concentration increases when the alkali concentration decreases. The decrease in the alkali content indicates a decrease in pH. Lowering of the pH of the pore solution in concrete is known to result in an increase in the calcium concentration (Lothenbach, 2010).

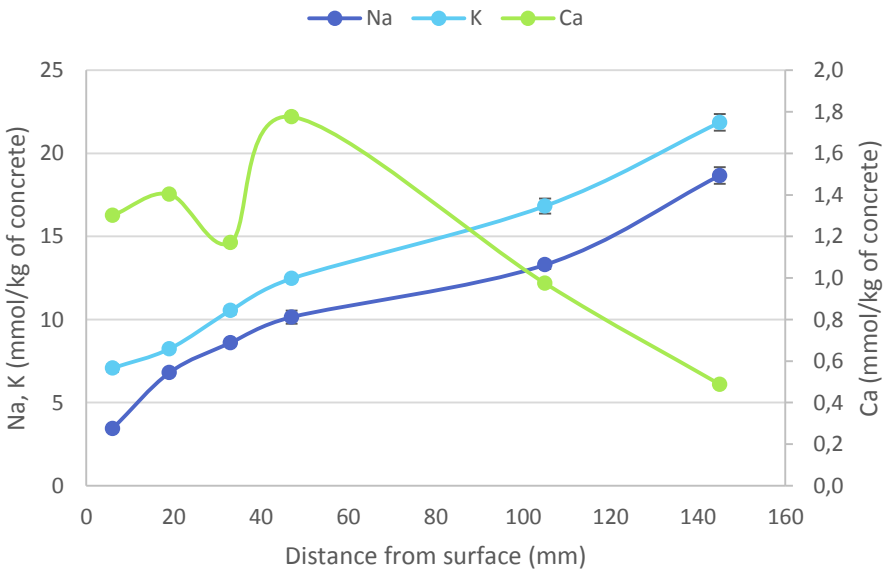

Figure 3.2: ICP results of core III-7 (permanently submerged on the upstream side).

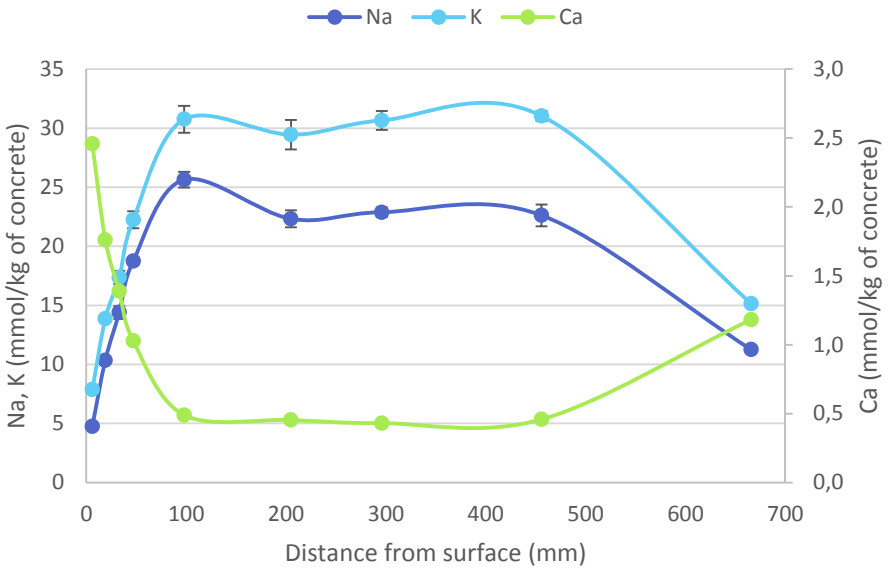

Figure 3.3: ICP results of core I-14 (permanently submerged on the upstream side).

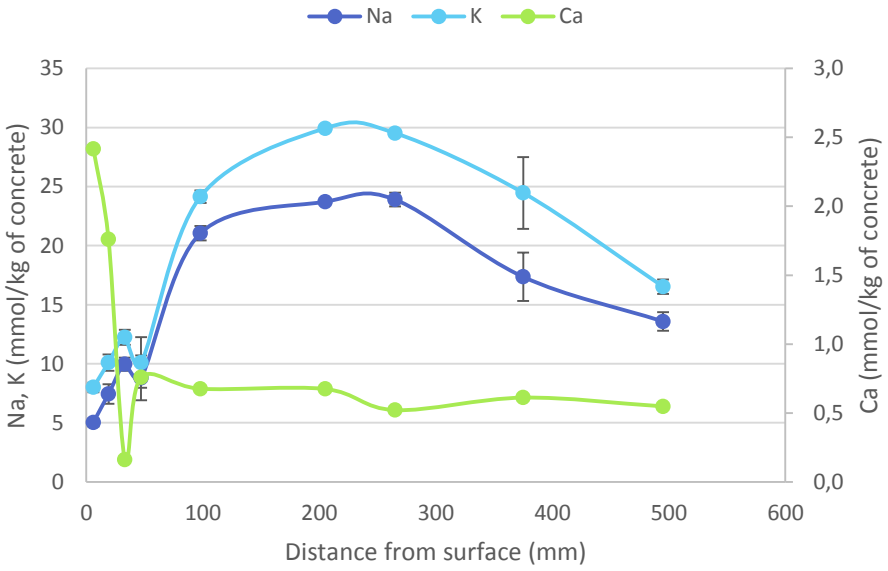

Figure 3.4: ICP results of core II-13 (partially submerged core on the upstream side).

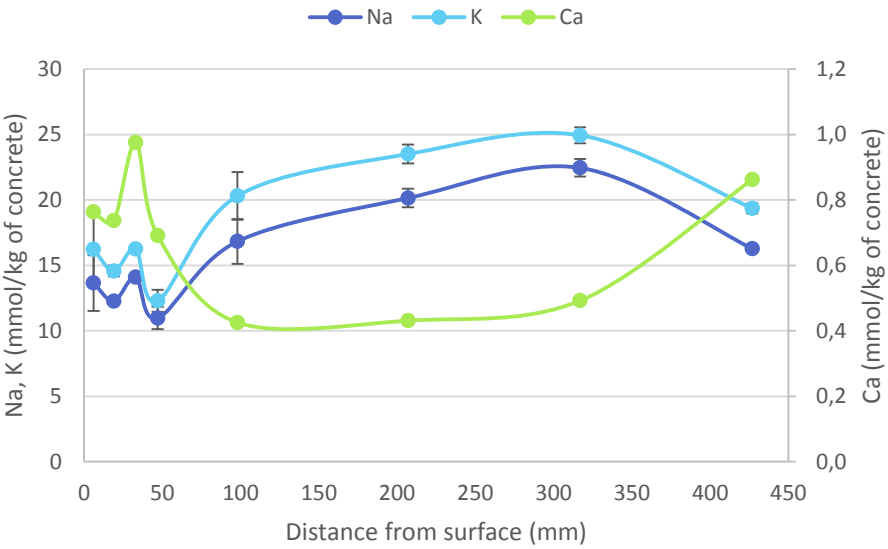

Figure 3.5: ICP results of core VI-2 (exposed to rain on the downstream side).

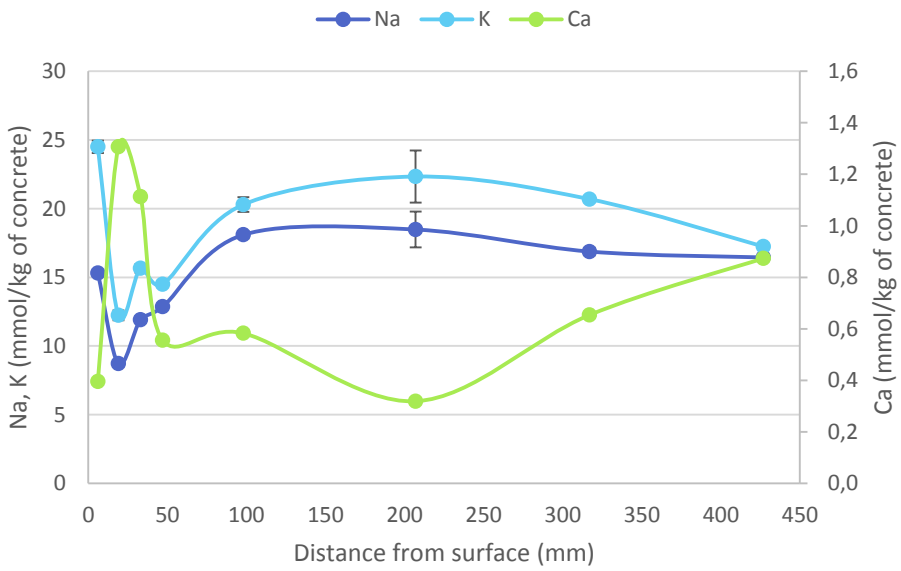

Figure 3.6: ICP results of core VII-5 (sheltered inside the dam).

Figure 3.7 and Figure 3.8 compare the concentration of respectively sodium (Na) and potassium (K) distributed on the length for different investigated cores. Both figures look very similar, which indicates that the Na and K profiles are interrelated. The most noticeable difference between these two graphs is that the concentration of potassium (K) is higher compared to the concentration of sodium (Na) for each core, which can be expected as the concentration of potassium always is higher than the concentration of sodium in Norwegian cement compositions. Core I-14 has a leaching depth up to 10 cm from the exposed surface, and core II-13 also seems to be similar. The plateau values for Na and K are similar for the concrete of core I-14 and core II-13.The sodium content lies between 20 and 25 mmol/kg of concrete (Figure 3.7) and the potassium content lies between 27 and 33 mmol/kg of concrete (Figure 3.8). Core I-14 and II-13 are taken from the same slab, which makes it very likely that the same concrete is used. On the other hand, the alkali content for core VI-2 which was exposed to rain and core VII-5 which was sheltered inside the dam, both taken from the pillar, also seem to be similar with each other. Level of alkali in these latter cores, core VI-2 and VII-5, lies between 20 and 25 mmol/kg of concrete for potassium (Figure 3.8) and around 20 mmol/kg of concrete for sodium (Figure 3.7). Hence, the cores taken from the pillar, core VI-2 and VII-5, seem to have slightly lower alkali contents compared to the cores taken from the slab, core I-14 and II-13. The assumption is therefore that one type of concrete is used for the slab while a different type of concrete is used at the outer pillar and inside the dam where respectively core VI-2 and VII-5 are taken from.

As mentioned, the ICP results involve both the release from the aggregates and paste. In order to estimate the potential alkali contribution from the aggregates, the paste content needs to be determined. This will be done in a follow up study.

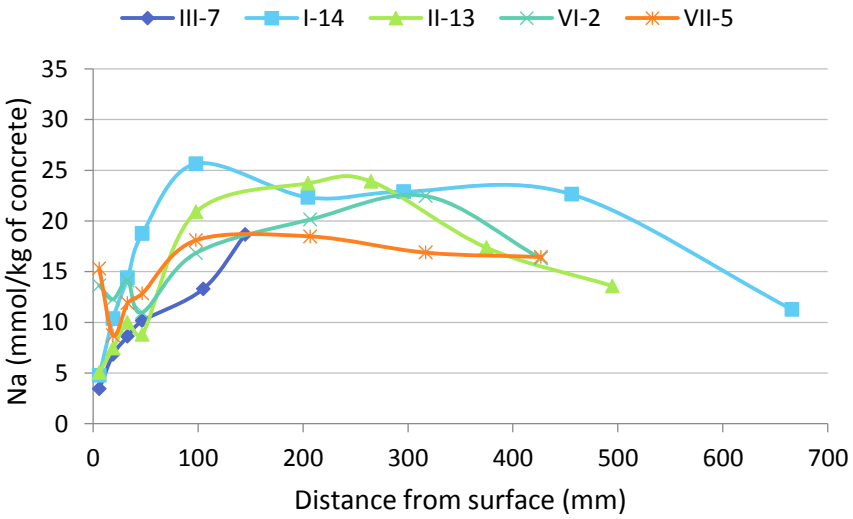

Figure 3.7: Na content for the different investigated concrete cores. The total length of the respective cores is 300 mm for III-7, 705 mm for I-14, 630 cm for II-13 and 480 mm for both VI-2 and VII-5.

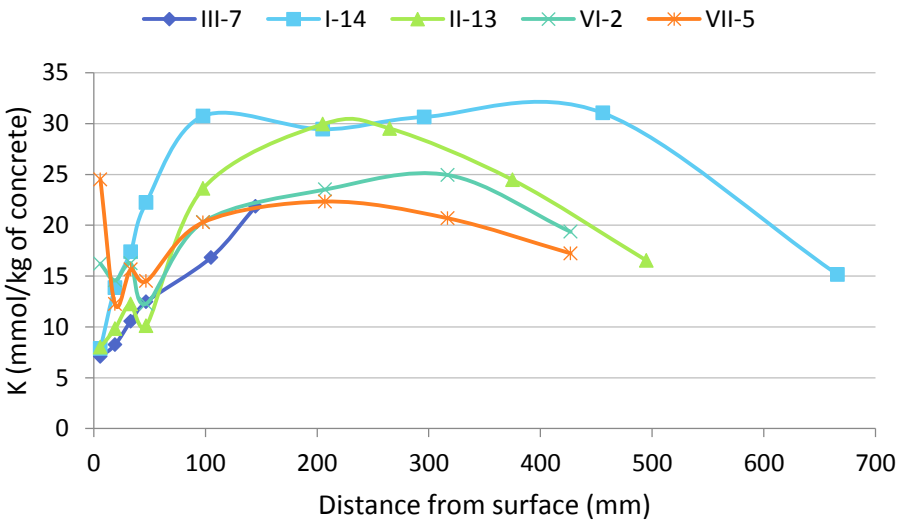

Figure 3.8: K content for the different investigated concrete cores. The total length of the respective cores is 300 mm for III-7, 705 mm for I-14, 630 cm for II-13 and 480 mm for both VI-2 and VII-5.

4. Conclusion

- Based on the obtained results, it is reasonable to conclude that the used method, Cold Water Extraction, is applicable to measure the leaching profile for the alkali ions, sodium (Na) and potassium (K) in in-situ concrete.
- The aggregates have an impact on the leaching. The calculations show that the alkali contribution in CWE test from the aggregates is at least 10 %, which is an important release. As it was not possible to remove the aggregates, their contribution is included in measured total alkali content.
- In the different investigated cores similar profiles are obtained for sodium and potassium. This proves that the concentration of sodium and potassium are interrelated, and indicates that both are affected by leaching.
- Due to the alkali content when comparing all the cores, it is possible to conclude that the concrete used at the slab, represented by core I-14 and II-13, is different from the concrete used at the outer pillar, core VI-2, and inside the dam, core VII-5.
- The depths of leaching and the leaching profiles are depending on the exposure conditions. For the submerged core I-14 and the partially submerged core II-13 the leached depth is up to 10 cm. The submerged core I-14 has the smoothest profile of leaching among all the cores, and also the clearest plateau. It is not possible to conclude the depth of leaching for the other submerged core III-7, which is only a part of a longer core. The received part for this study is too short to show a complete profile, but it indicates decrease of alkali ions towards the exposed surface. For core VI-2, which was exposed to rain, no clear leaching profile was observed. The core VII-5 sheltered inside the dam also indicates no leaching, as the alkali content from the outermost point at the surface is similar to the concentration of alkalis from the bulk concrete.

5. Further research

As a further research, it would be interesting to investigate the impact of leaching on damage development and structural behavior of in-situ structures. To the authors knowledge, ASR will be reduced where there is leaching as shown by Jan Lindgård from Sintef on laboratory samples (Lindgård, 2013a). Hence, if a formation of ASR gel occurs, it might occur inside the dam where there is no leaching.

Further research should be done on the quantification of the amount of aggregates and paste in the different slices to be able to correct for the alkali contribution. This can be done by for example using Thermogravimetric analysis (TGA).

The obtained alkali content should also be used to determine the pH of the pore solution. One should take into account the dilution which is induced by the addition of water during CWE. The concentration of Na and K is then calculated back in the original sample. Consequently, it is necessary to know the amount of pore solution in the sample before CWE. The pH can finally be determined with thermodynamic modelling software, as for example PhreeqC.

6. References

ALONSO, M., GARCÍA CALVO, J. & WALKER, C. 2012. Development of an accurate pH measurement methodology for the pore fluids of low pH cementitious materials. Swedish Nuclear Fuel and Waste Management Co., Stockholm (Sweden).

ANDERSSON, K., ALLARD, B., BENGTSSON, M. & MAGNUSSON, B. 1989. Chemical composition of cement pore solutions. *Cement and Concrete Research,* 19, 327-332.

ANDRADE, C., MERINO, P., NOVOA, X., PÉREZ, M. & SOLER, L. Passivation of reinforcing steel in concrete. Materials Science Forum, 1995. Trans Tech Publ, 891-898.

BARNEYBACK, R. S. & DIAMOND, S. 1981. Expression and analysis of pore fluids from hardened cement pastes and mortars. *Cement and Concrete Research,* 11, 279-285.

BÉRUBÉ, M.-A., DUCHESNE, J., DORION, J. & RIVEST, M. 2002a. Laboratory assessment of alkali contribution by aggregates to concrete and application to concrete structures affected by alkali–silica reactivity. *Cement and Concrete research,* 32, 1215-1227.

BÉRUBÉ, M.-A., FRENETTE, J., RIVEST, M. & VÉZINA, D. 2002b. Measurement of the alkali content of concrete using hot-water extraction. *Cement, concrete and aggregates,* 24, 28-36.

BOKERN, J. Concrete tests for ASR assessment: Effects of testing environment on preconditions for an ASR and transferability of test results. Proceedings of the 13th International Conference on Alkali-Aggregate Reactions in Concrete, Trondheim, Norway, 2008. 511-520.

CASTELLOTE, M., ALONSO, C., ANDRADE, C., CASTRO, P. & ECHEVERRIA, M. 2001. Alkaline leaching method for the determination of the chloride content in the aqueous phase of hardened cementitious materials. *Cement and Concrete Research,* 31, 233-238.

DESCHENES, D. J., BAYRAK, O. & FOLLIARD, K. J. 2009. ASR/DEF-damaged bent caps: shear tests and field implications. Citeseer.

DIAMOND, S. ASR—another look at mechanisms. Proceedings of the 8th International Conference on Alkali-Aggregate Reaction, Kyoto, Japan, 1989. 83-94.

DIAMOND, S. Chemistry and other characteristics of ASR gels. Proceedings of the 11th International Conference on Alkali-Aggregate Reaction in Concrete, Quebec City, Canada, 2000. 40.

DRON, R. & BRIVOT, F. 1992. Thermodynamic and kinetic approach to the alkali-silica reaction. Part 1: Concepts. *Cement and Concrete Research,* 22, 941-948.

DRON, R. & BRIVOT, F. 1993. Thermodynamic and kinetic approach to the alkali-silica reaction. Part 2: Experiment. *Cement and Concrete Research,* 23, 93-103.

FOURNIER, B. & BÉRUBÉ, M.-A. 2000. Alkali-aggregate reaction in concrete: a review of basic concepts and engineering implications. *Canadian Journal of Civil Engineering,* 27, 167-191.

FOURNIER, B., DUCHESNE, J., GOVETTE, S. & SANCHEZ, L. 2016. Evaluation of the alkali content in concrete through a modified hot-water extraction method. *15th ICAAR.* Sao Paulo, Brazil.

HAGELIA, P. Origin of map cracking in view of the distribution of air-voids, strength and ASR-gel. Proc. of the 12th Int. Conf. on AAR in Concrete, Beijing (China), 2004. 870-881.

HAUGEN, M., SKJØLSVOLD, O., LINDGÅRD, J. & WIGUM, B. J. 2004. Cost effective method for determination of aggregate composition in concrete structures. *12th ICAAR Conference, Beijing*.

JOHANSEN, S. 2009. *TKT 4215 Concrete Technology 1*, Trondheim, Norwegian University of Science and Technology.

LARSEN, S., LINDGÅRD, J., THORENFELDT, E., RODUM, E. & HAUGEN, M. Experiences from extensive condition survey and FEM-analyses of two norwegian concrete dams with ASR. Citeseer.

LI, L., NAM, J. & HARTT, W. H. 2005. Ex situ leaching measurement of concrete alkalinity. *Cement and concrete research,* 35, 277-283.

LI, L., SAGÜÉS, A. A. & POOR, N. 1999. In situ leaching investigation of pH and nitrite concentration in concrete pore solution. *Cement and Concrete Research,* 29, 315-321.

LINDGÅRD, J. 2013a. *Alkali-silica reaction (ASR) - Performance testing.* Doctor philosophiae Doctoral Thesis, Norwegian University of Science and Technology.

LINDGÅRD, J. 2013b. *Alkali-silica reaction (ASR)–Performance testing.* PhD, NTNU.

LINDGÅRD, J., WEERDT, K. D. & PLUSQUELLEC, G. 2015. Sampling plan Votna I dam.

LINGÅRD, J., CEPUTIRIS, R., HAUGEN, M., AARSTAD, K. & JACOBSEN, S. 2015. Chapter 9 - Concrete aggregates. *TKT 4215 Concrete Technology 1*.

LONGUET, P., BURGLEN, L. & ZELWER, A. 1973. La phase liquide du ciment hydraté. *Revue des Materiaux de construction,* 676, 35-41.

LOTHENBACH, B. 2010. Thermodynamic equilibrium calculations in cementitious systems. *Materials and structures,* 43, 1413-1433.

MULTON, S., SELLIER, A. & CYR, M. 2009. Chemo–mechanical modeling for prediction of alkali silica reaction (ASR) expansion. *Cement and Concrete Research,* 39, 490-500.

OPSAHL, M., GJERP, P. & SMEPLASS, S. 2005. *Grunneggende Betongteknologi*, Byggenæringens Forlag AS.

PAN, J., FENG, Y., WANG, J., SUN, Q., ZHANG, C. & OWEN, D. 2012. Modeling of alkali-silica reaction in concrete: a review. *Frontiers of Structural and Civil Engineering,* 6, 1-18.

PAVLIK, V. R. 2000. Water extraction of chloride, hydroxide and other ions from hardened cement pastes. *Cement and concrete research,* 30, 895-906.

PLUSQUELLEC, G., GEIKER, M., LINDGÅRD, J., WEERDT, K. D., FOURNIER, B. & DUCHESNE, J. 2016. Determination of the pH and the free alkali metals content in the pore solution of concrete: review and experimental comparison.

RAJABIPOUR, F., GIANNINI, E., DUNANT, C., IDEKER, J. H. & THOMAS, M. D. A. 2015. Alkali–silica reaction: Current understanding of the reaction mechanisms and the knowledge gaps. *Cement and Concrete Research,* 76, 130-146.

ROZIÈRE, E., LOUKILI, A., EL HACHEM, R. & GRONDIN, F. 2009. Durability of concrete exposed to leaching and external sulphate attacks. *Cement and Concrete Research,* 39, 1188-1198.

SAGÜÉS, A. A., MORENO, E. I. & ANDRADE, C. 1997. Evolution of pH during in-situ leaching in small concrete cavities. *Cement and Concrete Research,* 27, 1747-1759.

SELLEVOLD, E. J. & FARSTAD, T. The PF-method–A simple way to estimate the w/c-ratio and air content of hardened concrete. Proceedings of ConMat'05 and Mindess Symposium. Vancouver, Canada: The University of British Colombia. ISBN 0-88865-810-0, 2005.

7. Appendices

Table of content:

Appendix 1: The XRF composition

Table 7.1: The entire XRF composition

Sample marked	Aggregate powder
J.No.	160087
Fe2O3 (%)	2,61
TiO2 (%)	0,26
CaO (%)	0,87
K2O (%)	5,00
P2O5 (%)	0,03
SiO2 (%)	72,94
Al2O3 (%)	12,78
MgO (%)	0,28
Na2O (%)	2,86
MnO (%)	0,02
LOI (%) 1000°C	0,94
Total (%)	98,59

Appendix 2: The molecular mass of sodium, potassium and oxygen.

Table 7.2: The molecular mass of Na, K and O

Element	Molar mass (g/mol)
Na	22,99
K	39,10
O	16,00

Appendix 3: Calculation of the aggregate release

Table 7.3: Obtained results from the aggregate release

Washed samples	Conc. Na µg/L	Mean Value Na µg/L	Conc. K µg/L	Mean Value K µg/L
AW2	112 095	106 481	211 057	198 383
AW3	103 979		193 641	
AW4	103 369		190 452	

Na:

106,481 mg/L * 0,02 L = 2,1296 mg

2,1296 mg / 22,99 g/mol = 0,0926 mmol

0,0926 mmol /20 g = 0,00463 mmol/g ≈ 0,005 mmol/g

K:

198,383 mg/L * 0,02 L = 3,9677 mg

3,9677 mg / 39,10 g/mol = 0,1015 mmol

0,1015 mmol / 20 g = 0,005 mmol/g

Appendix 4: Composition of concrete in Votna 1

Table 7.4: Composition of the concrete in Votna 1

Area	Cement content	Sand content	Crushed rock content	Water content	Aggregate content
	kg/m3	kg/m3	kg/m3	kg/m3	%
8	331	970	959	170	39
3	326	950	949	165	40
I	331	968	961	170	40
II	332	961	962	175	40
II	333	965	963	169	40
7	333	965	958	154	40
13	330	948	957	165	40
9	330	958	959	163	40

This is just for documentation. To this date, the type of the concrete is unknown.

Appendix 5: Sampling of the concrete cores

CWE - Core III-7

Slices position (cut by sawing):

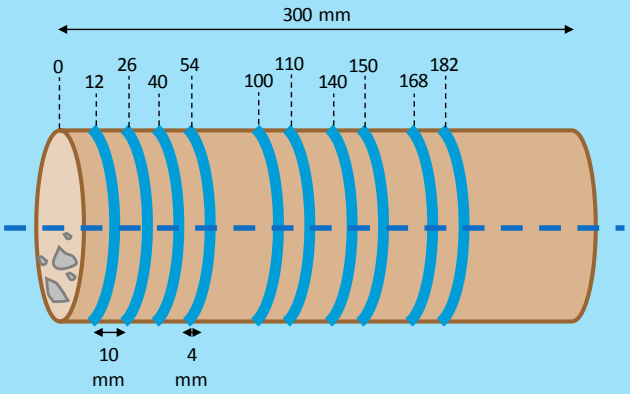

CWE details

Name	m powder (g)	m solvant (g)	Observation
III-7-1-A	20,004	20,005	Water
III-7-1-B	20,003	20,001	Water
III-7-1-C	20,001	20,002	Water
III-7-1-M	10,002	10,000	Methanol
III-7-2-A	20,001	20,002	Water
III-7-2-B	20,001	20,005	Water
III-7-2-C	20,002	20,006	Water
III-7-2-M	10,005	9,999	Methanol
III-7-3-A	20,001	20,007	Water
III-7-3-B	20,005	20,005	Water
III-7-3-C	20,004	20,003	Water
III-7-3-M	10,003	10,003	Methanol
III-7-4-A	20,001	20,003	Water
III-7-4-B	20,000	20,000	Water
III-7-4-C	20,003	20,004	Water
III-7-4-M	10,002	10,000	Methanol
III-7-5-A	20,002	20,003	Water
III-7-5-B	20,003	19,998	Water
III-7-5-C	20,000	19,998	Water
III-7-5-M	10,001	10,004	Methanol
III-7-6-A	20,002	20,005	Water
III-7-6-B	20,002	20,001	Water
III-7-6-C	20,003	20,003	Water
III-7-6-M	10,004	10,006	Methanol

Figure 7.1: Core III-7, details about slices and CWE.

CWE - Core I-14

Slices position (cut by sawing):

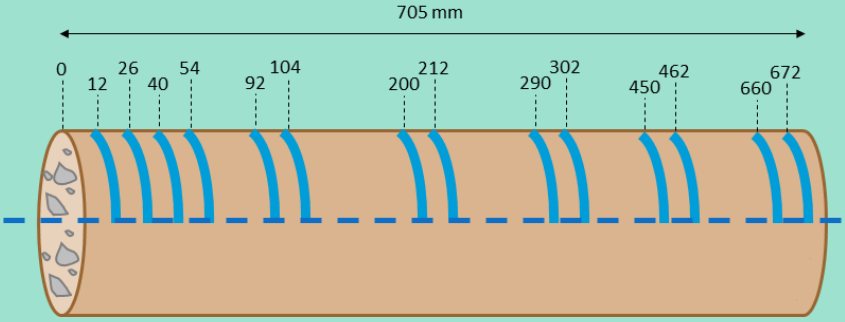

CWE details

Name	m powder (g)	m solvant (g)	Observation
I-14-1-A	20,002	20,004	Water
I-14-1-B	20,004	20,002	Water
I-14-2-A	20,002	19,999	Water
I-14-2-B	20,003	20,001	Water
I-14-3-A	20,002	20,000	Water
I-14-3-B	20,004	20,002	Water
I-14-4-A	20,003	20,002	Water
I-14-4-B	20,003	20,003	Water
I-14-5-A	20,004	20,001	Water; Approx. time
I-14-5-B	20,003	20,004	Water
I-14-6-A	20,002	20,004	Water
I-14-6-B	20,005	20,000	Water
I-14-7-A	20,002	19,998	Water
I-14-7-B	19,999	20,001	Water
I-14-8-A	20,002	19,999	Water
I-14-8-B	20,003	19,999	Water
I-14-9-A	20,001	20,007	Water
I-14-9-B	20,002	20,002	Water
I-14-1-M	9,998	10,002	Methanol
I-14-2-M	10,005	10,000	Methanol
I-14-3-M	10,001	10,002	Methanol
I-14-4-M	10,002	10,000	Methanol
I-14-5-M	10,002	10,005	Methanol
I-14-6-M	10,000	10,001	Methanol
I-14-7-M	10,003	10,004	Methanol
I-14-8-M	10,001	10,002	Methanol
I-14-9-M	10,005	10,006	Methanol

Figure 7.2: Core I-14, details about slices and CWE.

CWE - Core II-13

Slices position (cut by sawing):

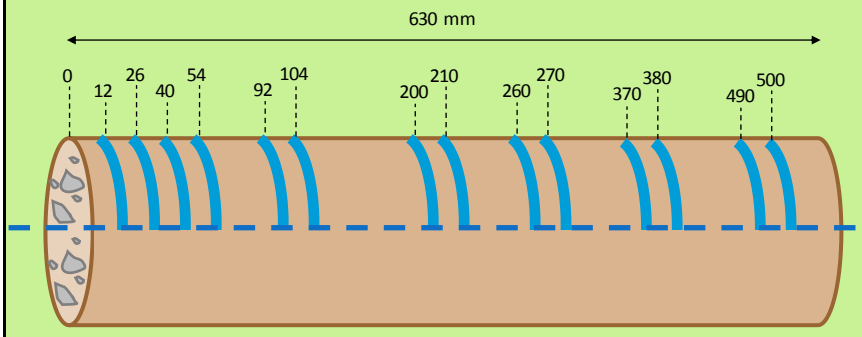

CWE details

Name	m powder (g)	m solvant (g)	Observation
II-13-1-A	20,000	20,000	Water
II-13-1-B	20,001	20,002	Water
II-13-2-A	20,002	20,004	Water
II-13-2-B	20,003	20,000	Water
II-13-3-A	20,005	20,005	Water
II-13-3-B	20,002	20,003	Water
II-13-4-A	20,000	20,005	Water
II-13-4-B	20,000	20,003	Water
II-13-5-A	20,001	20,000	Water
II-13-5-B	20,002	20,002	Water
II-13-6-A	20,002	20,005	Water
II-13-6-B	20,000	20,000	Water
II-13-7-A	20,002	20,005	Water
II-13-7-B	20,003	20,003	Water
II-13-8-A	20,002	20,003	Water
II-13-8-B	20,001	20,001	Water
II-13-9-A	20,001	20,001	Water
II-13-9-B	20,002	20,000	Water
II-13-1-M	10,001	10,004	Methanol
II-13-2-M	10,001	9,999	Methanol
II-13-3-M	10,001	10,000	Methanol
II-13-4-M	10,004	10,002	Methanol
II-13-5-M	10,003	10,001	Methanol
II-13-6-M	10,003	10,005	Methanol
II-13-7-M	10,003	10,004	Methanol
II-13-8-M	10,003	9,999	Methanol
II-13-9-M	10,001	10,002	Methanol

Figure 7.3: Core II-13, details about slices and CWE.

CWE - Core VI-2

Slices position (cut by sawing):

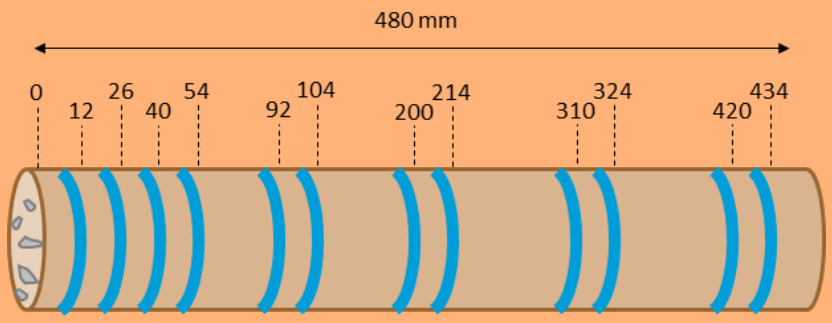

CWE details

Name	m powder (g)	m solvant (g)	Observation
VI-2-1-A	20,001	20,000	Water
VI-2-1-B	20,001	20,002	Water
VI-2-2-A	20,002	20,001	Water
VI-2-2-B	20,002	20,000	Water
VI-2-3-A	20,001	20,003	Water
VI-2-3-B	20,002	20,004	Water
VI-2-4-A	20,003	20,004	Water
VI-2-4-B	20,002	20,002	Water
VI-2-5-A	20,000	20,002	Water
VI-2-5-B	20,000	19,999	Water
VI-2-6-A	20,000	20,002	Water
VI-2-6-B	20,000	20,000	Water
VI-2-7-A	20,003	20,001	Water
VI-2-7-B	20,000	20,003	Water
VI-2-8-A	20,002	19,999	Water
VI-2-8-B	20,002	20,004	Water
VI-2-1-M	10,001	10,003	Methanol
VI-2-2-M	10,000	10,002	Methanol
VI-2-3-M	10,002	10,001	Methanol
VI-2-4-M	10,000	10,002	Methanol
VI-2-5-M	10,001	10,001	Methanol
VI-2-6-M	10,001	10,003	Methanol
VI-2-7-M	10,000	10,000	Methanol
VI-2-8-M	10,001	10,003	Methanol

Figure 7.4: Core VI-2, details about slices and CWE.

CWE - Core VII-5

Slices position (cut by sawing):

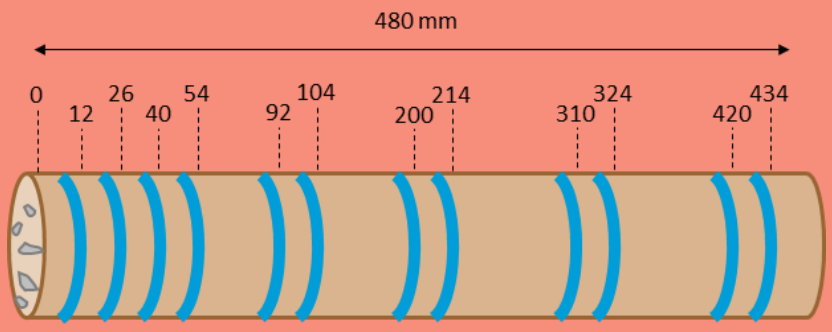

CWE details

Name	m powder (g)	m solvant (g)	Observation
VII-5-1-A	20.002	20.002	Water
VII-5-1-B	20.002	20.003	Water
VII-5-2-A	20.003	20.007	Water
VII-5-2-B	20.002	20.003	Water
VII-5-3-A	20.004	20.006	Water
VII-5-3-B	20.008	20.009	Water
VII-5-4-A	20.002	20.005	Water
VII-5-4-B	20.005	20.006	Water
VII-5-5-A	20.003	20.007	Water
VII-5-5-B	20.003	20.003	Water
VII-5-6-A	20.004	20.004	Water
VII-5-6-B	20.005	20.004	Water
VII-5-7-A	20.006	20.006	Water
VII-5-7-B	20.005	20.001	Water
VII-5-8-A	20.001	20.005	Water
VII-5-8-B	20.002	20.003	Water
VII-5-1-M	10.004	10.004	Methanol
VII-5-2-M	10.003	10.002	Methanol
VII-5-3-M	10.004	10.000	Methanol
VII-5-4-M	10.002	10.003	Methanol
VII-5-5-M	10.004	10.005	Methanol
VII-5-6-M	10.006	10.004	Methanol
VII-5-7-M	9.999	10.000	Methanol
VII-5-8-M	10.003	10.001	Methanol

Figure 7.5: Core VII-5, details about slices and CWE.

Appendix 6: The abstract for the 2nd Nordic mini – seminar

2nd Nordic mini-seminar on Residual service life & capacity of deteriorated concrete structures

HiOA Oslo, 1st and 2nd of June 2016

ASR in Votna dam – alkali leaching

Havvagul Vurucu, Klaartje De Weerdt, Mette R. Geiker, Gilles Plusquellec

NTNU, Department of Structural Engineering, Trondheim, Norway

Abstract

This study focuses on the Votna 1 dam, which is a double curved arch dam connected to a slab-dam. The dam is situated in the south – western part of Norway 950 m above sea level and was constructed in the years between 1964 and 1966. It was first in 1987 – 1988 that map cracking, typical for alkali silica reaction (ASR), was observed at Votna 1. After deformation measurements at the top of the arch dam one could confirm that ASR had started.

ASR occurs only if three conditions are fulfilled: alkali reactive aggregate, high pH in the pore solution and high moisture content. Under these conditions, alkali – silica gel may form. This gel may absorb water and swell. This volume increase in the concrete makes the concrete expand and results in a characteristic crack pattern at the surface called map cracking.

The objective of this study is to understand the possible influence of the exposure conditions on the pH of the pore solution of the concrete. The hypothesis is that the pH will be reduced due to leaching of alkalis near the surface on the water exposed site of the dam. This could lead to differential expansion between leached and non-leached part of the dam.

Summer 2015, concrete cores (Φ 150 mm) were retrieved from a selection of locations at the slab-dam with different exposure conditions: permanently submerged, submerged only part of the year, above the water level exposed to rain, and sheltered inside the dam. The extent of leaching for the different exposure conditions is investigated by measuring the alkali metal profiles using the cold water extraction – method.

Figure 7.6: The typical map cracking pattern at Votna 1 (Photo: Gilles Plusquellec).